

# Contact of screw surfaces with displaced axes

V. Machulda<sup>a</sup>, J. Švígler<sup>a,\*</sup>

<sup>a</sup>Faculty of Applied Sciences, UWB in Pilsen, Univerzitiní 22, 306 14 Plzeň, Czech Republic

Received 23 July 2010; received in revised form 20 December 2011

---

## Abstract

A couple of conjugate screw surfaces, which create a three-member mechanism with a higher kinematic pair, constitutes an important part of mechanical systems. One of these surfaces is created as an envelope of the second surface. In an ideal arrangement surface axes are parallel and the contact between both surfaces is curvilinear. After displacement of the surface axes, which is induced in technical equipments by force and heat loading, the original parallel arrangement of the surface axes is changed into an incorrect, spatial or alternatively parallel displaced, position. Consequently the original curvilinear contact changes into a contact at a point. This change is significant from the view of contact analysis. Determination of the contact point of conjugate surfaces, which are in the incorrect position, based on the kinematic way is presented in this contribution.

© 2011 University of West Bohemia. All rights reserved.

*Keywords:* conjugate screw surfaces, kinematic method, contact point, axes displacement

---

## 1. Introduction

Let us consider two conjugate surfaces. In theory the arrangement of surface axes is usually parallel and the contact between conjugate screw surfaces is curvilinear. However owing to external influences the original parallel position of surface axes acquires an incorrect configuration. As a consequence the original curvilinear contact is changed into a contact at a point. This change influences force loading between the surfaces and their relative motion. The original relative rolling motion changes into a spatial motion that can be described with kinematic screw, twist [4]. Ascertaining the contact between conjugate surfaces is described for example in [1, 3]. In [1] the solution is based upon differential approach and in [3] a spatial problem is simplified. For using the solution from [3] it is necessary to consider a minor displacement of axes. In this contribution the kinematic method of determining a contact point of conjugate surfaces is presented. The kinematic method, which is based on Disteli principle [2], is highly illustrative and provides an effective solution of the problem. The kinematic way is very suitable for arbitrarily generated surfaces, thus not only for the conjugate screw surfaces, which are only a special case of general surfaces. The presented solution can be used for any displacement of axes. The solution is divided into two steps. In the first step a parallel displacement of surface axes is considered. In the second step general displacement is taken into consideration. In this paper the matrix notation of the kinematic analysis is made in homogeneous coordinates in this paper. Let be remarked an arrangement of axes of considered surfaces with curvilinear contact can be, in a theoretical case, arbitrary.

---

\*Corresponding author. Tel.: +420 377 632 324, e-mail: svigler@kme.zcu.cz.

## 2. Creation of conjugate surfaces

### 2.1. Creating surface $\sigma_2$

Let us consider profile  $p_2$  of creating surface  $\sigma_2$  as an arc of circle, which is described in coordinate system  $R_{2\gamma}$ , Fig. 1, with equation

$${}_{R_{2\gamma}}\mathbf{r}_L^{\sigma_2}(\chi) = \begin{bmatrix} {}_{R_{2\gamma}}x_L^{\sigma_2} \\ {}_{R_{2\gamma}}y_L^{\sigma_2} \\ {}_{R_{2\gamma}}z_L^{\sigma_2} \\ 1 \end{bmatrix} = \begin{bmatrix} r_S \sin \Phi - r_K \sin \chi \\ -r_S \cos \Phi + r_K \cos \chi \\ 0 \\ 1 \end{bmatrix}, \quad (1)$$

where  ${}_{R_{2\gamma}}\mathbf{r}_L^{\sigma_2}$  is the position vector of point  $L \in p_2$  and  $r_S, r_K, \Phi, \chi$  are geometric parameters. Surface  $\sigma_2(\psi_2, \chi)$ , which is two parametric manifold, is created by screw motion of profile  $p_2$  along surface axis  $o_2$ . This screw motion, which is equivalent to transformation from coordinate system  $R_{2\gamma}$  to  $R_2$ , is described with equation

$${}_{R_2}\mathbf{r}_L^{\sigma_2}(\psi_2, \chi) = \mathbf{T}_{R_{2\gamma}, R_2} {}_{R_{2\gamma}}\mathbf{r}_L^{\sigma_2}(\chi) = \begin{bmatrix} \cos \psi_2 & -\sin \psi_2 & 0 & 0 \\ \sin \psi_2 & \cos \psi_2 & 0 & 0 \\ 0 & 0 & 1 & \delta_2 \\ 0 & 0 & 0 & 1 \end{bmatrix} {}_{R_{2\gamma}}\mathbf{r}_L^{\sigma_2}(\chi), \quad (2)$$

where  ${}_{R_{2\gamma}}\mathbf{r}_L^{\sigma_2}(\chi)$  is the position vector of profile point  $L \in \sigma_2$ ,  $\delta_2 = r_{W2}\psi_2 \tan \gamma$  is the displacement along the surface axis  $o_2$ ,  $r_{W2}$  is the radius of rolling cylinder and  $\gamma$  is the helix angle on the rolling cylinder. With the use of (2) the creating surface  $\sigma_2$  is, in coordinate system  $R_2$ , defined as

$${}_{R_2}\mathbf{r}_L^{\sigma_2}(\psi_2, \chi) = \begin{bmatrix} r_S \sin (\Phi + \psi_2) - r_K \sin (\chi + \psi_2) \\ -r_S \cos (\Phi + \psi_2) + r_K \cos (\chi + \psi_2) \\ \delta_2 \\ 1 \end{bmatrix}. \quad (3)$$

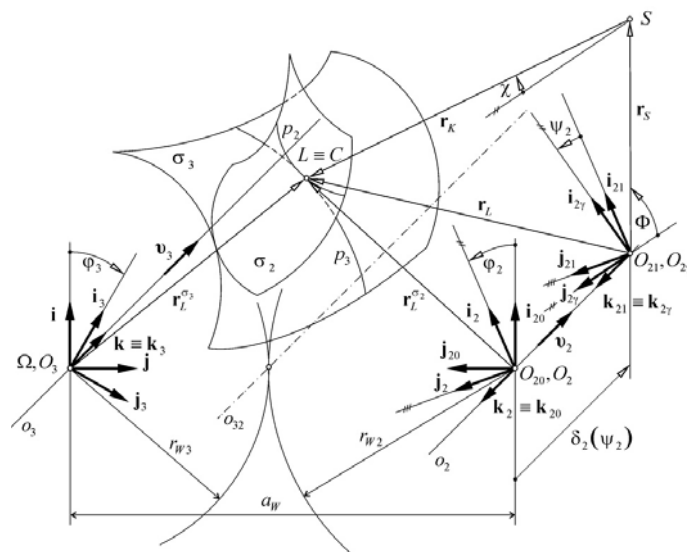


Fig. 1. Creation of conjugate surfaces  $\sigma_2$  and  $\sigma_3$

### 2.2. Conjugate surface $\sigma_3$

Creating conjugate surface  $\sigma_3$  is based, as mentioned above, on Disteli principle. A solution presupposes the fact, that contact point  $L \equiv L^{\sigma_2} \equiv L^{\sigma_3} \equiv C$  is a common point of both surfaces for an instantaneous position of angular displacement  $\varphi_2$ . In the basic coordinate system  $R \equiv (i, j, k)$ , see Fig. 1, the contact point has to comply with two conditions

$${}_R r_L^{\sigma_3} = {}_R r_L^{\sigma_2}, \tag{4}$$

$$\mathbf{n}_L \cdot \mathbf{v}_{L32} = 0, \tag{5}$$

where  ${}_R r_L^{\sigma_3}$  is the position vector of point  $L \in \sigma_3$ ,  ${}_R r_L^{\sigma_2}$  is the position vector of point  $L \in \sigma_2$ ,  $\mathbf{n}_L$  is the normal vector in point  $L$  and  $\mathbf{v}_{L32}$  is the vector of the relative velocity in point  $L$ . The normal vector  $\mathbf{n}_L$  can be defined as a cross product of the tangent vectors to the profile  $p_2$  in point  $L$  and to the helix through point  $L$ . The vector of the relative velocity can be defined as difference between the vector of velocity of surface  $\sigma_3$  and the vector of velocity of surface  $\sigma_2$  in the same point  $L$ .

With the use of transformation matrices equation (4) can be written as

$${}_{R_3} r_L^{\sigma_3} = \mathbf{T}_{R,R_3} \mathbf{T}_{R_20,R} \mathbf{T}_{R_2,R_20} {}_{R_2} r_L^{\sigma_2} \tag{6}$$

and substituting (3) into (6) we obtain

$${}_{R_3} r_L^{\sigma_3}(\psi_2, \varphi_2, \chi) = \begin{bmatrix} r_S \sin(\Phi + \varphi_2 + \varphi_3 + \psi_2) - r_K \sin(\chi + \varphi_2 + \varphi_3 + \psi_2) + a_W \sin \varphi_3 \\ r_S \cos(\Phi + \varphi_2 + \varphi_3 + \psi_2) - r_K \cos(\chi + \varphi_2 + \varphi_3 + \psi_2) + a_W \cos \varphi_3 \\ \delta_2 \\ 1 \end{bmatrix}. \tag{7}$$

Equation (5) represents the condition of perpendicularity of normal vector  $\mathbf{n}_L$  and vector of the relative velocity  $\mathbf{v}_{L32}$  in contact point  $L \equiv C$  of surfaces  $\sigma_2$  and  $\sigma_3$ . Equation (5) can be rewritten, on condition that the profile  $p_2$  is created by an arc of a circle, into form

$$(i_{32} + 1) \cdot r_K \sin(\chi - \Phi) + a_W \sin(\varphi_2 + \chi + \psi_{2L}) = 0, \tag{8}$$

where  $a_W$  is the distance between axes  $o_2, o_3$  and  $i_{32} = \frac{\omega_3}{\omega_2} = \frac{\varphi_3}{\varphi_2}$  is a gear ratio. Equation (8) represents functional relationship  $f(\varphi_2, \chi) = 0$ . Using equations (7) and (8) conjugate surface  $\sigma_3$  is determined as two dimensional manifold  $f(\psi_2, \chi) = 0$ .

### 3. Contact of surfaces with displaced axes

The variation of the position of surface axes entails a displaced position of conjugate surfaces, which must be taken into consideration. As a result of this phenomenon an alternation of the surface contact takes place. Theoretical accurate contact, referred to as “correct contact”, changes into incorrect contact. The incorrect contact is solved for two cases of arrangement of displaced axes. In the first case, a parallel displacement of axes is studied. In the second step, a general displacement of axes is taken into consideration.

#### 3.1. Parallel displacement of axes

The incorrect contact of screw surfaces is caused by parallel displacement of the axes which were inserted, by fixed axis  $o_3$ , in the axis  $o_2$ . Subsequently axis  $o_2$  is shifted in new, deformed,



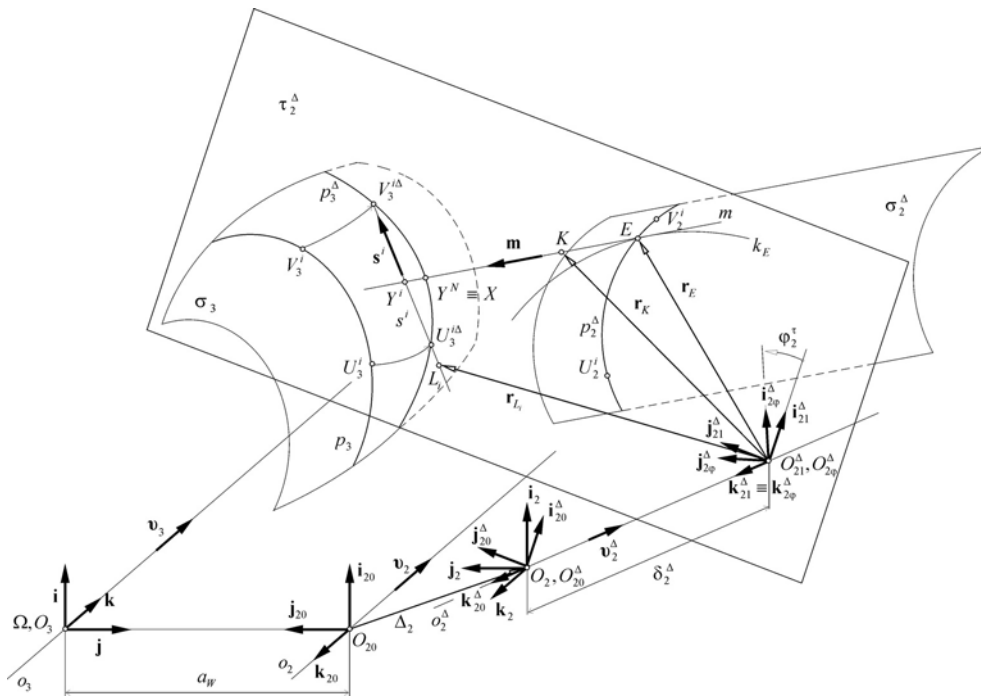


Fig. 3. Determination of contact point of profile  $p_3^\Delta$  and  $p_2^\Delta$  in cross section  $\tau_2^\Delta$

equation (8) and angle  $\varphi_{3K0}$  determines the position of surfaces  $\sigma_3$  and  $\sigma_2^\Delta$ . With the use of (10) line  $s^i$ , Fig. 2, can be defined as

$$\mathbf{r}_{L_i} = \mathbf{r}_{U_3^i} + q(\mathbf{r}_{V_3^i} - \mathbf{r}_{U_3^i}) = \mathbf{r}_{U_3^i} + q\mathbf{s}^i, \quad (11)$$

where  $L_i \in s^i$ ,  $s^i$  is the directional vector of a secant  $s^i$  and  $q$  is a parameter. Using equations (9) and (11) we obtain vector equation for determination of point of intersection  $Y^i \in s^i$  with line  $m$  as

$$\mathbf{r}_E + p\mathbf{m} - \mathbf{r}_{U_3^i} - q\mathbf{s}^i = \mathbf{0}. \quad (12)$$

Interval bisection method is used for the determination of parameters  $\chi^{A_i}$  of points  $U_3^i$  and  $V_3^i$  in the next iteration step. The iterative process continues until  $U_3^N \equiv V_3^N \equiv X$ . In the next step surface  $\sigma_2^\Delta$  is gradually turned around axis  $o_2^\Delta$  until  $p = 0$ , where  $p$  is a parameter determined by equation (12). Then  $E \equiv X \wedge X \equiv m \cap p_3$ . This algorithm is applied on all points of creating surface  $\sigma_2^\Delta$  and the contact of surfaces  $\sigma_3$  and  $\sigma_2^\Delta$  is achieved under condition

$$\mathbf{r}_L^{\sigma_2^\Delta} \equiv \mathbf{r}_E \equiv \mathbf{r}_X \equiv \mathbf{r}_L^{\sigma_3} \wedge \mathbf{n}_L^{\sigma_3} \equiv \mathbf{n}_L^{\sigma_2^\Delta} \wedge \varphi_2^\tau = \min \varphi_2^\tau \quad (13)$$

and then  $L \equiv C$ .

### 3.2. General displacement of axes

In this case the arrangement of axes is generally skewed. Similarly, as in the case of parallel displacement of axes, axis  $o_3$  is fixed and axis  $o_2$  is shifted into new, deformed, position  $o_2^\Delta$  and surface  $\sigma_2$  is displaced in position  $\sigma_2^\Delta$ , Fig. 3. The determination of the contact point  $C$  of surfaces  $\sigma_3$  and  $\sigma_2^\Delta$  is based on the solution for the parallel displaced axes. The main distinction consists in the fact that plane  $\tau_2^\Delta$ , where contact of profiles  $p_3^\Delta \equiv \sigma_3 \cap \tau_2^\Delta$  and  $p_2^\Delta \equiv \sigma_2^\Delta \cap \tau_2^\Delta$  is solved, is not perpendicular to axis  $o_3$  and profile  $p_3^\Delta$  differs from profile  $p_3$  of surface  $\sigma_3$

in the cross section which is perpendicular to axis  $o_3$ . Analogous to the case with parallel displaced axes the solution is divided into two steps. In the first step the determination of point  $X \equiv m \cap p_3^{\tau_2^\Delta} \wedge X \equiv Y^N, Y^N \in \{Y^i\}$ , where  $m$  is tangent to circle  $k_E$  which passes through chosen point  $E \in p_2^\Delta$  and  $Y^i \equiv m \cap s_i$ , is achieved. In the second step creating surface  $\sigma_2^\Delta$  is gradually turned around axis  $o_2^\Delta$  until  $E \equiv X \wedge X \equiv m \cap p_3^\Delta \equiv Y^N$ . The solution is made in coordinate system  $R_{20}^\Delta \equiv (\mathbf{i}_{20}^\Delta, \mathbf{j}_{20}^\Delta, \mathbf{k}_{20}^\Delta)$ .

Analogous to the previous case, an iterative method was used for the determination of point  $X \equiv Y^N$ . General point  $K$  of tangent  $m$  is determined by equation

$$\mathbf{r}_K = \mathbf{r}_E + p\mathbf{m}, \tag{14}$$

where  $\mathbf{m}$  is the unit vector of line  $m$  and  $p$  is a parameter. For determination of secant  $s_i$  of profile  $p_3^\Delta$  points  $U_3^{i\Delta}, V_3^{i\Delta} \in \sigma_3 \wedge U_3^{i\Delta}, V_3^{i\Delta} \in \tau_2^\Delta, i = 1 \div n$ , are necessary to use. The position vectors of these points are determined by equation

$${}_{R_{20}^\Delta} \mathbf{r}_{A_3^{i\Delta}} = \begin{bmatrix} {}_{R_{20}^\Delta} x_{A_3^{i\Delta}} \\ {}_{R_{20}^\Delta} y_{A_3^{i\Delta}} \\ {}_{R_{20}^\Delta} z_{A_3^{i\Delta}} \\ 1 \end{bmatrix} = \mathbf{T}_{R, R_{20}^\Delta} \begin{bmatrix} \cos \Delta\psi_3 & -\sin \Delta\psi_3 & 0 & 0 \\ \sin \Delta\psi_3 & \cos \Delta\psi_3 & 0 & 0 \\ 0 & 0 & 1 & \Delta\delta_3 \\ 0 & 0 & 0 & 1 \end{bmatrix} {}_R \mathbf{r}_{A_3^i}, \tag{15}$$

where  $A_3^{i\Delta} \equiv U_3^{i\Delta}, V_3^{i\Delta}, A_3^i \equiv U_3^i, V_3^i$  are points of profile  $p_3$  which position vectors  ${}_R \mathbf{r}_{A_3^i}$  are determined by equation (10).  $\Delta\delta_3 = r_{W3} \Delta\psi_3 \tan \gamma$  is the displacement along the surface axis  $o_3$  and angle  $\Delta\psi_3$  is determined by equation

$${}_{R_{20}^\Delta} z_{A_3^{i\Delta}} = \delta_2^\Delta. \tag{16}$$

Using points  $U_3^{i\Delta}, V_3^{i\Delta}$  general point  $L_i$  of secant  $s_i$  is defined as

$$\mathbf{r}_{L_i} = \mathbf{r}_{U_3^{i\Delta}} + q(\mathbf{r}_{V_3^{i\Delta}} - \mathbf{r}_{U_3^{i\Delta}}) = \mathbf{r}_{U_3^{i\Delta}} + q\mathbf{s}^i, \tag{17}$$

where  $L_i \in s^i, \mathbf{s}^i$  is the directional vector of secant  $s^i$  and  $q$  is a parameter.

Using equations (14) and (17) intersection  $Y^i \in s^i$  with line  $m$  is determined as solution of equation

$$\mathbf{r}_E + p\mathbf{m} - \mathbf{r}_{U_3^{i\Delta}} - q\mathbf{s}^i = \mathbf{0}. \tag{18}$$

The rest of the solution to the iteration and process of gradual turning of surface  $\sigma_2^\Delta$  are analogous as in the case of parallel displaced axes and contact of surfaces  $\sigma_3$  and  $\sigma_2^\Delta$  is obtained under condition

$${}_{R_{20}^\Delta} \mathbf{r}_L^{\sigma_2^\Delta} \equiv {}_{R_{20}^\Delta} \mathbf{r}_E \equiv {}_{R_{20}^\Delta} \mathbf{r}_X \equiv {}_{R_{20}^\Delta} \mathbf{r}_L^{\sigma_3} \wedge \mathbf{n}_L^{\sigma_3} \equiv \mathbf{n}_L^{\sigma_2^\Delta} \wedge \varphi_2^\tau = \min \varphi_2^\tau \tag{19}$$

and then  $L \equiv C$ .

## 4. Application

### 4.1. Application to simple screw conjugate surfaces

For application, creating surface  $\sigma_2$ , Fig. 1, with geometric parameters  $r_S = 45$  mm,  $\Phi = \frac{2}{3}\pi$  rad,  $r_K = 30$  mm,  $\gamma = \frac{1}{4}\pi$  rad,  $r_{W2} = a_W / (1 + 1/i_{32})$ , where  $a_W = 100$  mm and  $i_{32} = 0.75$ , was considered. Domains of the definition of surface parameters are  $\chi \in \langle 0; \frac{\pi}{3} \rangle$  rad,  $\psi_2 \in \langle 0; 1 \rangle$  rad.

Using equations (3), (7) and (8) creating surface  $\sigma_2$  and conjugate surface  $\sigma_3$  are determined. In the first case, the parallel displacement of axes was considered. Displacement of creating surface was stated  $\Delta_2 = [1; 2; 0]^T$  mm. With the use of the algorithm mentioned in section 3.1, contact point of surfaces  $\sigma_2^\Delta$  and  $\sigma_3$  was determined for three positions of surfaces defined by angle  $\varphi_{3K0} = -10^\circ, 0^\circ, 10^\circ$ . Dependence of  $\min \varphi_2^T$ , equation (19), on displacement  $\delta_2$  along axis  $o_2^\Delta$  of surface  $\sigma_2^\Delta$  is shown in Fig. 4. A variation of the position of contact point  $C$  of conjugate surfaces  $\sigma_2^\Delta, \sigma_3$  depending on setting up conjugate surfaces is shown in Fig. 5. Fig. 6 presents a shifting of contact point  $C$  on surface  $\sigma_3$ , for surface arrangement mentioned above, which is situated in position  $\varphi_{3K0} = 0^\circ$ .

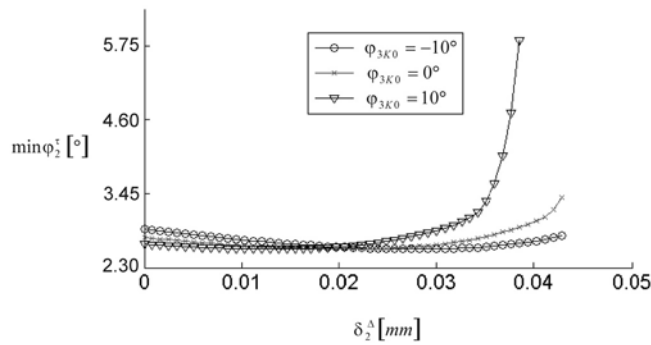


Fig. 4. Dependence of  $\min \varphi_2^T$  on  $\delta_2^\Delta$

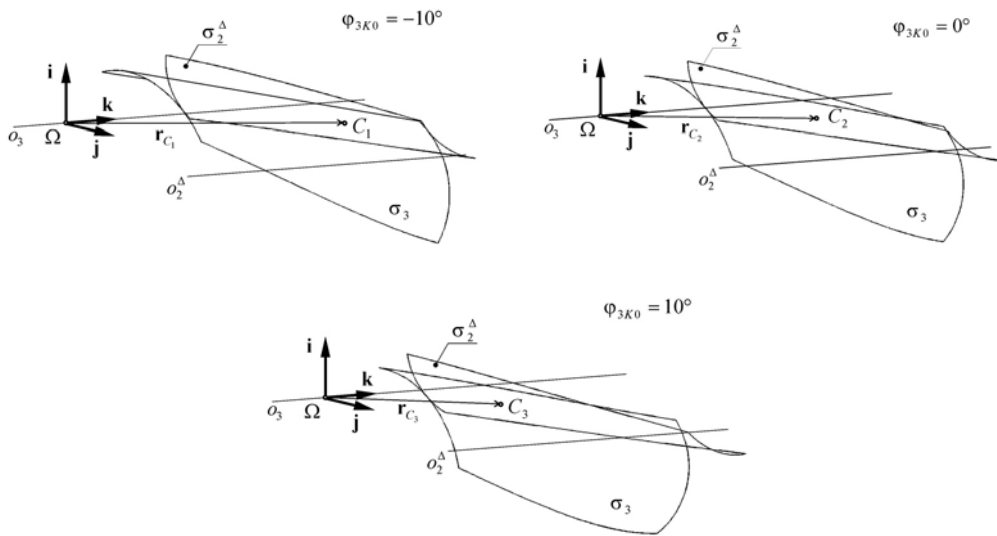


Fig. 5. Positions of contact point  $C$  of conjugate surfaces  $\sigma_2^\Delta$  and  $\sigma_3$

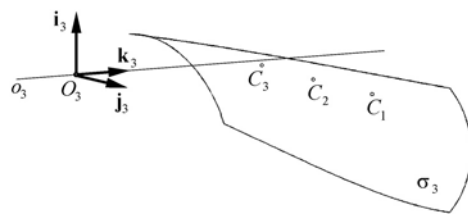


Fig. 6. Displacement of contact point  $C$  on surface  $\sigma_3$

Let us consider the identical couple of conjugate surfaces as in the previous case but for a spatial arrangement. Skew arrangement of axes is determined by displacement of creating surface  $\sigma_2$  in frontal plane  $\Delta_2 = [1; 2; 0]^T$  mm of axis  $o_2$  and the unit direction vector of axis  $\nu_2^\Delta = [0.0250; -0.0499; 0.9984]^T$ . The algorithm described in section 3.2 was applied to considered case of conjugate surfaces and dependence of angle  $\min \varphi_2^T$  on the displacement along axis  $o_2^\Delta$  of surface  $\sigma_2^\Delta$  is shown in Fig. 7. A variation of contact point  $C$  depending on the rotary angle of conjugate surfaces is presented in Fig. 8 and shifting of the same contact point on surface  $\sigma_3$  is shown in Fig. 9 where the position  $C_1 \div C_3$  corresponds to the position of the same points in Fig. 8.

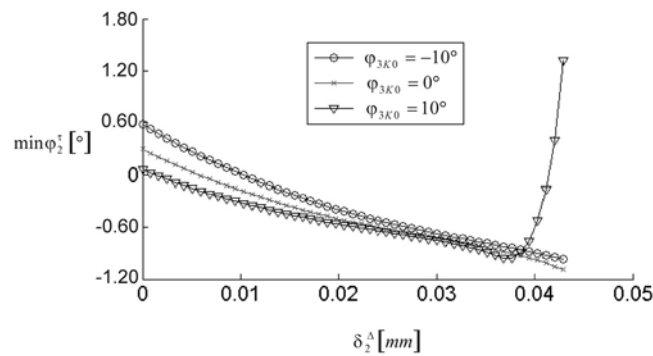


Fig. 7. Dependence of  $\min \varphi_2^T$  on  $\delta_2^\Delta$

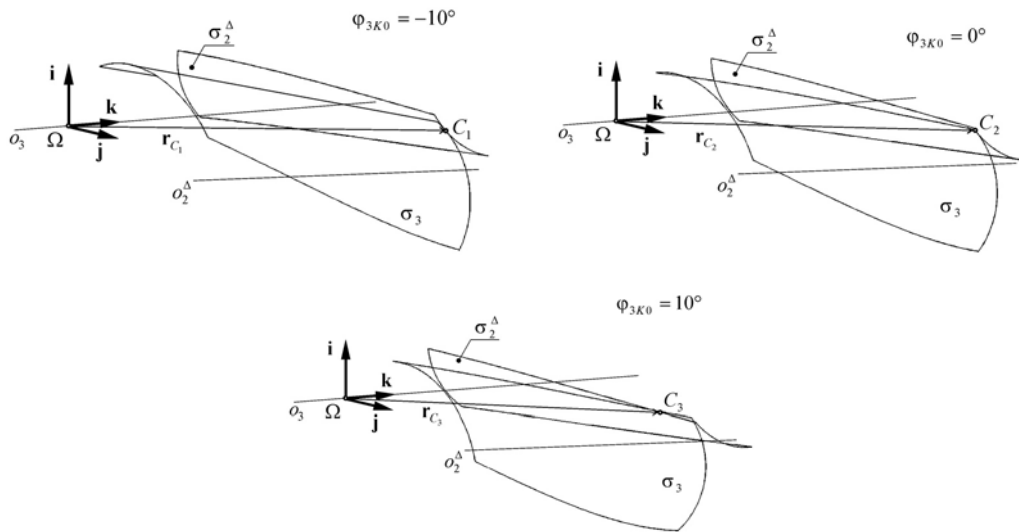


Fig. 8. Positions of contact point  $C$  of conjugate surfaces  $\sigma_2^\Delta$  and  $\sigma_3$

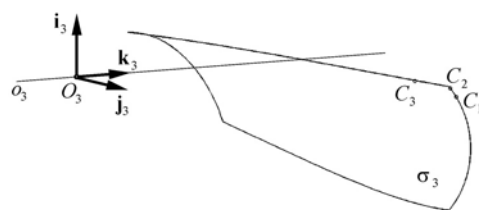


Fig. 9. Displacement of contact point  $C$  on surface  $\sigma_3$

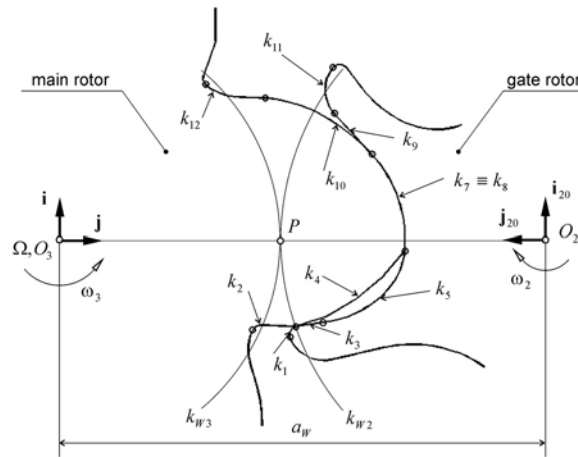


Fig. 10. Profiles of conjugate tooth surfaces

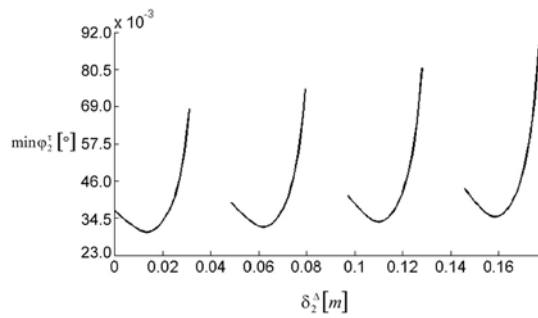


Fig. 11. Dependence of  $\min \varphi_2^\tau$  on  $\delta_2^\Delta$

#### 4.2. Application to tooth surfaces of screw compressor

Tooth surfaces of the screw compressor with the profile SLF4 were considered in the case of application of the presented method to real technical equipment with conjugate surfaces. The main parameters of the compressor rotors are the following. The distance between axes  $a_W = 85$  mm, gear ratio  $i_{32} = 5/6$ , helix angle on the rolling cylinders  $\gamma = \pi/4$  rad and the length of toothed part of rotors  $l = 193.8$  mm. Tooth surface  $\sigma_2$  of the gate rotor, which is the creating surface, consists of several single surfaces that are interconnected continuously and smoothly. Profiles of the considered tooth surfaces in the frontal section are shown in Fig. 10. Creating curves of the profile of the gate rotor are arcs of circles  $k_1$ ,  $k_3$ ,  $k_7$  and  $k_{11}$ , arc of trochoid  $k_5$  and straight line  $k_9$ . A tooth profile of the main rotor consists of curves  $k_2$ ,  $k_4$ ,  $k_8$ ,  $k_{10}$  and  $k_{12}$ , which are envelopes of mentioned creating curves of the gate rotor. For contact analysis the meshing parts of the profiles, which are defined by curves  $k_7$ ,  $k_9$  and  $k_{11}$  of the gate rotor and conjugate curves  $k_8$ ,  $k_{10}$  and  $k_{12}$  of the main rotor, are considered. Skew arrangement of rotor axes was defined by displacement of the gate rotor in frontal plane  $\Delta_2 = [1; 2; 0]^T$  mm and the unit direction vector of axis  $o_2^\Delta$  of gate rotor  $\nu_2^\Delta = [0.010\ 3; 0.005\ 2; 0.999\ 9]^T$ . First of all, the contact of surfaces in a position defined by angle  $\varphi_{3K0} = 0^\circ$  was solved. Dependence of  $\min \varphi_2^\tau$  on displacement  $\delta_2^\Delta$  along axis  $o_2^\Delta$  is presented in Fig. 11 for this case. For analysis of the contact of tooth surfaces  $\sigma_3$ ,  $\sigma_2^\Delta$  during an operating cycle, which is given by a turning about one tooth pitch of the main rotor, the domain of definition of angular displacement of the main rotor is  $\varphi_{3K0} \in \langle 0^\circ, 72^\circ \rangle$ . Displacement of contact point  $C$  of the  $p$ -th pair of teeth on tooth

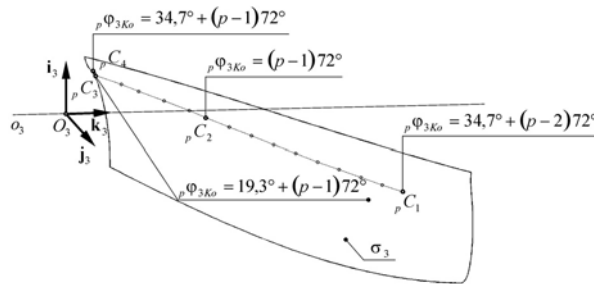


Fig. 12. Translation of contact point on surface  $\sigma_3$  of the main rotor

surface  $\sigma_3$  of the main rotor is shown in Fig. 12. Point  ${}_pC_1$  is the point where the contact of the  $p$ -th pair of teeth starts. Point  ${}_pC_2$  determines the position in which the contact point conforms to the starting position of both surfaces, Fig. 12, upon their creating. Point  ${}_pC_3$  determines the first point in frontal cross-section,  ${}_p\varphi_{3K0} = 19.3^\circ + (p-1)72^\circ$ , where contact of tooth surfaces  $\sigma_3, \sigma_2^\Delta$  of considered  $p$ -th pair is made and point  ${}_pC_4$  is the last contact point of the  $p$ -th pair of teeth in frontal plane,  ${}_p\varphi_{3K0} = 34.7^\circ + (p-1)72^\circ$ .

## 5. Conclusion

As a result of external influences such as force, temperature and dynamic loading in mechanical systems the original arrangement of surfaces is shifted into a displaced position. This change causes a variation of the characteristics of the contact of surfaces and their relative motion. The originally relative rolling motion changes into the general spatial motion, which is given by relative twist, and the curve contact of surfaces changes into the contact at point. The presented method makes it possible to establish the instantaneous point of contact of conjugate surfaces which are in a deformed, incorrect position, in general. This circumstance is of extraordinarily important for contact analysis and dynamic analysis of mechanic systems or their parts in an operating state. For the afore mentioned reason the determination and specification of the incorrect contact of conjugate screw surfaces with displaced axes represents the first step for the following analysis. The presented method is suitable for arbitrary surfaces which are in contact.

## Acknowledgements

The work has been supported by the research project MSM 4977751303.

## References

- [1] Bär, G., Explicit Calculation Methods for Conjugate Profiles, Journal for Geometry and Graphics 7(2) (2003) 201–210.
- [2] Disteli, M., Über instantane Schraubengeschwindigkeiten und die Verzahnung der Hyperboloidräder, Zeitschrift für Mathematic und Physic Bd 53, 1904, p. 51–88. (in German)
- [3] Kameya, H., Aoki, M., Nozawa, S., Three-dimensional curvature analysis on screw rotor and its applications, Proceedings of the International Conference on Compressors and their Systems 2005, London, John Willey & Sons, LTD, 2005, p. 467–474.
- [4] Švejl, M., Applied kinematics spatial gear transmission, Doctoral thesis, Pilsen, 1967. (in Czech)